Single Conducting Polymer Nanowire Based Sequence-Specific, Base-Pair-Length Dependant Label-free DNA Sensor

Mangesh A. Bangar,[a] *Dhammanand J. Shirale*,[a, b] *Hemant J. Purohit*,[c] *Wilfred Chen*,[a] *Nosang V. Myung*,[a] *Ashok Mulchandani**[a]

[a] Chemical and Environmental Engineering, University of California, Riverside, Riverside, CA 92521, USA
[b] Currently at Vellore Institute of Technology, Vellore, Tamilnadu, India
[c] Environmental Genomics Unit, National Environmental Engineering Research Institute, CSIR, Nagpur, Maharashtra 440020, India
*e-mail: adani@engr.ucr.edu

Received: June 24, 2010
Accepted: September 22, 2010

Abstract
We have fabricated a highly sensitive, simple and label-free single polypyrrole (Ppy) nanowire based conductometric/chemiresistive DNA sensor. The fabrication was optimized in terms of probe DNA sequence immobilization using a linker molecule and using gold-thiol interaction. Two resultant sensor designs working on two different sensing mechanisms (gating effect and work function based sensors) were tested to establish reliable sensor architecture with higher sensitivity and device-to-device reproducibility. The utility of the work function based configuration was demonstrated by detecting 19 base pair (bp) long breast cancer gene sequence with single nucleotide polymorphism (SNP) discrimination with high sensitivity, lower detection limit of $\sim 10^{-16}$ M and wide dynamic range ($\sim 10^{-16}$ to 10^{-11} M) in a small sample volume (30 μL). To further demonstrate the utility of the DNA sensor for detection of target sequences with different number of bases, targets with 21 and 36 bases were detected. These sequences have implications in environmental sample analysis or metagenomics. Sensor response showed increase with the number of bases in the target sequence. For long sequence (with 36 bases), effect of DNA alignment on sensor performance was studied.

Keywords: Conducting polymer nanowire, DNA sensor, Gating effect, Work function difference, Breast cancer, Metagenomics, Nanowires

DOI: 10.1002/elan.201000388

1 Introduction

Point of care/use detection for personal health, safety and security as well as environmental monitoring using compact, field deployable sensors is gaining a lot of importance in research arena. Amongst different target analytes, DNA detection has immense importance due to its applications in personal health, forensic, mutations/disease diagnostics, drug discovery, food technology, and environmental sample analysis/metagenomics. Thus DNA sensors play an important role in numerous fields aimed at improving our lives. Sensitivity, selectivity, response time and sensor-to-sensor reproducibility of these sensors is strongly dictated by the sensor design, transduction method and sensing mechanism. Most of the conventional DNA detection strategies like PCR [1] and high throughput gene chips [2] are based on optical detection of DNA sequence/hybridization event. In an alternate technique, DNA probes are integrated with nanoparticles that exhibit changes in optical signal upon target DNA binding. Such method can be employed in an array format as well [3,4]. Surface plasmon resonance (SPR) based sensors report changes in the refractive index of a thin metal film upon target binding and is suitable for array application [5]. Techniques employing change in mass or associated physical changes in the sensor such as quartz-crystal microbalance [6] and cantilever [7] sensors are shown to be very sensitive. On the other hand, sensors employing electrochemical detection convert bio-recognition event directly into an electrical signal, which can be read using inexpensive electrochemical analyzer and has immense potential for miniaturization [8]. Such electrochemical sensors for DNA hybridization detection have been fabricated using metal electrodes [9,10], nanoparticles [11,12], carbon nanotubes [13,14], semiconductor nanowires such as GaN nanowires [15] or conducting polymers [16–20]. These sensors have shown excellent sensitivity, selectivity up to single base pair mismatch discrimination and ability to function in real samples with very little or no loss of performance.

Particularly of our interest, a true label-free, easy to use sensor for DNA detection has been demonstrated from class of sensors utilizing electrical signal based chemiresistive or field-effect transistor (FET) architecture. Due to direct conversion of biomolecule recognition event into an electrical signal, they offer fast, real-time and easy transduction along with easy miniaturization using modern day electronics. Use of nanomaterials has

been shown to improve performance and portability of these devices. Silicon nanowire based electrical detection for DNA using chemiresistor/FET design has been well studied [21–27]. Lately, carbon nanotube (CNT) has been nanomaterial of choice for DNA sensor fabrication amongst scientific community [28–31]. For these nanomaterial based sensors two different mechanisms have been suggested to effect the sensing performance of the sensor. First sensing mechanism is based on the sensitivity of the nanomaterials to their surface environment, especially to the presence of ions/charged analytes, referred to as gating effect. The second effect is based on the change in the alignment of energy levels of metal electrode and semiconducting nanochannel caused by change in the metal work function, referred to as Schottky barrier effect. A detailed discussion is presented in Reference [32], wherein protein absorption on carbon nanotube has been studied. However, different research groups have reported either of these two mechanisms as the dominant sensing mechanism depending upon the analyte (gaseous/liquid, DNA/protein) or even the operating temperature [29,32,33], thus making it necessary to identify a reliable sensor design and mechanism for given nanomaterial and the target analyte, in order to understand and improve sensor functioning.

Conducting polymers due to their excellent electrical properties, biocompatibility and functionalization chemistries, can function both as a semiconducting channel between the metal contact electrodes as well as the immobilization site for probe DNA. This would allow precise control on the sensor architecture and hence sensor characteristics and mechanism. Despite their easy synthesis, processibility, excellent material and electrical properties and obvious economical advantages, use of conducting polymer nanostructures has been limited for FET applications due to their incompatibility with traditional lithographic techniques owing to their possible thermal damages. Very few chemiresistor or FET applications have been demonstrated using these novel nanostructures due to their unstable metal/polymer junction under liquid environment [19,20,34–38]. To address this issue, we recently developed a facile method of fabricating single polypyrrole (Ppy) nanowire based sensors [36]. Single nanowire based devices offer excellent understanding and control of the device properties, sensor architectures and sensing mechanisms as against nanowire/tube-network based devices. Using this technique, in this study, we have studied two different probe ssDNA immobilization approaches and two resultant sensor architectures and mechanisms (gating vs. Schottky) to determine the most reliable and sensitive chemiresistive DNA sensor architecture and its performance. To demonstrate the utility of the sensor we have shown use of these sensors for the detection of human breast cancer gene with SNP (single nucleotide polymorphism) discrimination and detection of target DNA sequences with varying number of bases that are of interest in metagenomics studies currently ongoing at the National Environmental Engineering Research Institute, India. Further we have studied the effect of DNA alignment on the sensor performance.

2 Experimental

Sensor fabrication is adopted from our previously reported study on immunosensor using single nanowire based chemiresistive architecture [36]. Various steps involved in the process are as follows:

2.1 Nanowire Synthesis

Ppy nanowires were electrochemically deposited inside an alumina template with 200 nm nominal pore diameter and about 60 μm thickness (Whatman International Ltd., Maidstone, UK). One face of the template was sputter-coated with ~200 nm thick gold using the Emitech K550 (Emitech Ltd., Kent, UK) sputter coater. The electrodeposition was carried out in a three-electrode electrochemical cell with Ag/AgCl (3 M KCl) as a reference electrode, platinum-coated titanium strip as a counter electrode, and alumina template with the gold bottom-seed layer (~0.64 cm^2) as a working electrode using an EG&G PAR VMP2, (Princeton Applied Research, Tennessee) potentio/galvanostat. 0.5 M pyrrole in 0.2 M $LiClO_4$ solution at pH 6.3 that was purged with 99.99% nitrogen for 30 min before deposition was used as the electrolyte. Ppy nanowires were deposited potentiostatically at 0.9 V versus Ag/AgCl for 15 min. The overdeposited Ppy was mechanically polished away and the template was washed with water and acetone. Gold seed layer was etched away using 0.15 M KI in 0.1 M I_2 solution. After washing the template with water, alumina template was dissolved in 30% (v/v) H_3PO_4 acid. Solution was briefly sonicated to free the nanowires and form a suspension. The nanowires were subsequently washed with water three times before suspending them in 1.5 mL of water. The suspension was diluted 10-fold for further use.

2.2 Single Nanowire Based Device Assembly

Prefabricated gold microelectrodes made up of an array of 16 pairs of electrodes with rectangular electrodes of ~55 μm width separated by a 3 μm gap and ~70 μm separation between adjacent pairs were used as contact electrodes for device assembly. The two sides of 16 pairs were shorted to form two terminals and an alternating current (ac) field of 5 MHz and 1 V peak-to-peak voltage was applied between these terminals. A 2 μL drop of Ppy nanowire suspension was dispensed on it, and alignment was carried out. Using a probe tip made out of 25 μm diameter gold wire and a 1000× magnification optical microscope excess nanowires were physically/manually removed to obtain single-nanowire connection between a pair of contact electrodes. Finally a three-electrode electrochemical cell consisting of the 16 pairs of contact electrodes with single Ppy nanowire connections as the work-

ing electrode, Ag/AgCl as a reference electrode, and a platinum-coated metal strip as a counter electrode was used to selectively deposit gold on the 16 pairs of contact electrodes to anchor the nanowires. Using Technigold (Technic Inc., California) electrolyte at pH of 7.0, and the deposition potential of −0.5 V versus Ag/AgCl at room temperature for 10 min, ~300 nm thick gold layer was deposited on the gold electrode surface.

2.3 Thiol Modified 5′ DNA Probe Preparation

Following probe ssDNA sequences with 5′ thiol modifications and varying number of base pairs were purchased from Integrated DNA Technologies, Inc.

PR1 (19 bp):
HS-$(CH_2)_6$-5′-GAT TTT ATT CCT TTT GTT C-3′
PR2 (21 bp):
HS-$(CH_2)_6$-5′-TCG GTC ATG GAG ATC AGG TCG-3′
PR3 (36 bp):
HS-$(CH_2)_6$-5′-TCC CAG TTG GCG AAA ATC AGG CCC TTG TAG GTC TCC-3′

As purchased ssDNA probes contained S-S double bond at the 5′ end and were reduced by adding 0.1 M DTT (Sigma-Aldrich) for at least 12 hours. Reduced thiol end group containing ssDNA probe sequences were isolated from the reaction products with DTT using a desalting column.

2.4 Target Probes

Target ssDNAs with complementary or non-complementary sequence were purchased from Integrated DNA Technologies, Inc.

Complementary sequences:

TG1 (19 bp):
3′-CTA AAA TAA GGA AAA CAA G-5′
TG2 (21 bp):
3′-AGC CAG TAC CTC TAG TCC AGC-5′
TG3 (36 bp):
3′-AGG GTC AAC CGC TTT TAG TCC GGG AAC ATC CAG AGG-5′

Single, double and triple bp mismatched target sequences for PR1, respectively:

MU2 (19 bp):
3′-CTA AAA TAA GGA AAA **T**AA G-5′
MU12 (19 bp):
3′-CTA AAA TAA **T**GA AAA **T**AA G-5′
MU123 (19 bp):
3′-CTA AAA **C**AA **T**GA AAA **T**AA G-5′

2.5 Sensor Fabrication: Probe DNA Immobilization

Probe ssDNA sequences were immobilized either on the Ppy nanowire surface using a linker molecule, Succinimidyl 4-[*p*-maleimidophenyl]butyrate (SMPB) or on the gold surface using protocols explained below.

2.5.1 SMPB Linker Chemistry

To block the gold surface of the sensor, devices were incubated with 10% mercaptohexanol (MCH) overnight followed by immobilization of probe ssDNA on the Ppy nanowire surface using either of the following protocols.

One-step chemistry: Single nanowire devices were incubated with 20 μL of 10 mM SMPB and 20 μL of probe ssDNA solution each in 10 mM PB (phosphate buffer) at pH 7.2 (2 h). Devices were further washed with 0.1% Tween-20 containing PB (PBT) three times followed by washing with PB three times.

Two-step chemistry: Single nanowire devices were incubated with 20 μL of 10 mM SMPB (2 h). Excess SMPB was removed by washing the devices with PB three times. SMPB activated devices were incubated with probe ssDNA solution (2 h). Excess probe DNA solution was removed and devices were washed with PBT followed by PB three times each.

2.5.2 Gold Surface Immobilization

Single nanowire devices were directly incubated with 50 μL of probe ssDNA solution for about 24 hours. Excess solution was removed followed by washing with PBT and PB three times each.

2.5.3 DNA Alignment Control with MCH

DNA sensors with probe ssDNA immobilized on gold electrode surfaces were incubated with MCH solution for 1 h to remove non-specifically adsorbed probe ssDNA molecules from the gold surface as well as to orient the probe ssDNA molecules vertically that are attached to the gold electrode surface through gold-thiol interaction.

2.5.4 Blocking

Sensor functionalized with probe ssDNA were further blocked by incubating with 1 mg/mL of BSA (bovine serum albumin) solution in PB for 1 h. Control sample was blocked with BSA without carrying out probe ssDNA immobilization.

2.6 Chemiresistive Sensing Measurements

Sensor resistances were measured in terms of their current-voltage (*I–V*) responses using a semiconductor parameter analyzer (Model 4155A, Agilent Technologies Inc., CA) under wet conditions (with a 30 μL drop of PB on the nanowire). The voltage was swept from −200 to +200 mV across pair of contact electrodes and the current was recorded. The nanowire resistance was measured as the inverse of the slope of *I–V* near zero voltage in the linear range of ±100 mV. Resistance changes of the sensor upon exposure to different concentrations of target ssDNA sequences in 10 mM PB were measured in wet condition (with a 30 μL drop of PB on the nanowire)

after the sensor was incubated in respective analyte solution for 5 min followed by washing with PBT, followed by PB.

3 Results and Discussion

3.1 Breast Cancer Gene Detection

For breast cancer gene sequence (TG1) detection, its complementary DNA sequence PR1 was employed as the probe. A simple chemiresistive sensor configuration was used as a sensor architecture wherein single conducting polymer (polypyrrole, Ppy) nanowire was connected across the electrode gap between a pair of gold electrodes. Probe PR1 was immobilized on the sensor surface and the sensor was exposed to very small volume (30 μL) of different target DNA sequences. The response of the sensor towards target DNA sequences was recorded as a change in the nanowire resistance (R). This change (ΔR) was normalized with respect to the initial sensor resistance (R_0) to establish a basis to compare sensor to sensor reproducibility.

The immobilization efficiency of probe DNA has pronounced implication on the sensor performance. Thus identification of optimum immobilization strategy is important. We compared two approaches for immobilization of thiolated DNA probe on Ppy nanowire-based devices. In the first approach DNA probes were immobilized on the semiconducting Ppy nanowire bridging the two gold electrode pads that also acts as the transducer (Figure 1A). Such sensor configuration relies heavily on the gating effect in presence of the target. The presence of charged target on the semiconductor surface modulates the electrical properties of the nanowire such as resistance, which can be easily read without the need for any labeling. Succinimidyl 4-[*p*-maleimidophenyl]butyrate (SMPB) was used to link the thiolated probe oligonucleotide to the Ppy secondary amine-group as shown in Scheme 1. In order to prevent any interaction between thiolated PR1 and gold contact electrodes, gold electrodes were first blocked by mercaptohexanol (MCH). Two different protocols, one-step and two-steps, were compared. In a one-step protocol, nanowire devices were incubated with both linker molecules and the probe DNA (PR1) at the same time while in the two-steps protocol the nanowire surface was first activated with SMPB linker followed by immobilization of the PR1 ssDNA. To avoid nonspecific binding of the target oligonucleotide to the sensor surface, nonfunctionalized sites were blocked using bovine serum albumin (BSA). Irrespective of the protocol followed sensor with initial resistances in the range of 100 KΩ to 5 MΩ showed response towards its perfectly complementary target, TG1. Sensors with resistance lower than 100 KΩ showed almost no response whereas sensors with resistance higher than 5 MΩ showed very high sample to sample variation (data not shown). Thus, sensors with initial resistances in the 100 KΩ to 5 MΩ window were compared for their performance. The one-step protocol resulted in bigger sample to sample variation and the response did not scale with target concentration very well (data not shown). On the other hand, sensors fabricated with two-steps protocol resulted in a better response towards target DNA concentration that was scalable with target concentration over a wide dynamic range (10^{-15} to 10^{-11} M) [based on average sensor response trend] and a limit of detection of 10^{-15} M (Figure 1C) [based on sensor response (S) with target ssDNA vs. sensor response to solution without target ssDNA (N), $S/N > 3$]. Thus, it can be inferred that the immobilization efficiency achieved through the two-steps protocol was higher than that achieved by the one-step protocol resulting in a better sensor performance. However, a higher sample to sample variation (as evident from the error bars) can severely limit the utility of this type of sensor.

In the second DNA probe immobilization approach, PR1 was immobilized on the gold electrodes, thereby restricting the Ppy nanowire function to conduction channel only. Due to this simple change in the immobilization site from nanowire surface to contact/anchoring electrodes, such device geometry relies on the modulation of work function difference between the metal contact and the semiconducting Ppy nanowire brought about by the presence of target. As schematically represented by the energy diagram in Figure 2B, the change of work function of the metal upon target DNA hybridization with the probe DNA results in the modulation of the energy barrier (Schottky barrier) between the metal and the nanowire [29]. This can be easily detected by measuring the electrical resistance of the device before and after the hybridization. Two sensor designs, one in which unfunctionalized surfaces were blocked with BSA and the other without BSA blocking were compared. As shown in Figure 2, the sensor response/sensitivity in absence of BSA blocking (Figure 2A) was higher compared to the sensor with BSA blocking (Figure 2B). However, sensors blocked with BSA showed much lower sensor to sensor variation, i.e. better reproducibility, because of the effective blockage of non-specific binding/adsorption of target DNA on to

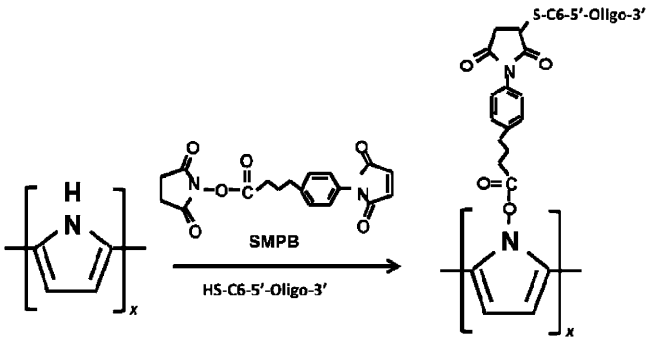

Scheme 1. Reaction schematic for linker molecule succinimidyl 4-[*p*-maleimidophenyl]butyrate (SMPB). Secondary amine from the polypyrrole backbone is connected to the thiol group on one end of the probe ssDNA sequence using this linking chemistry.

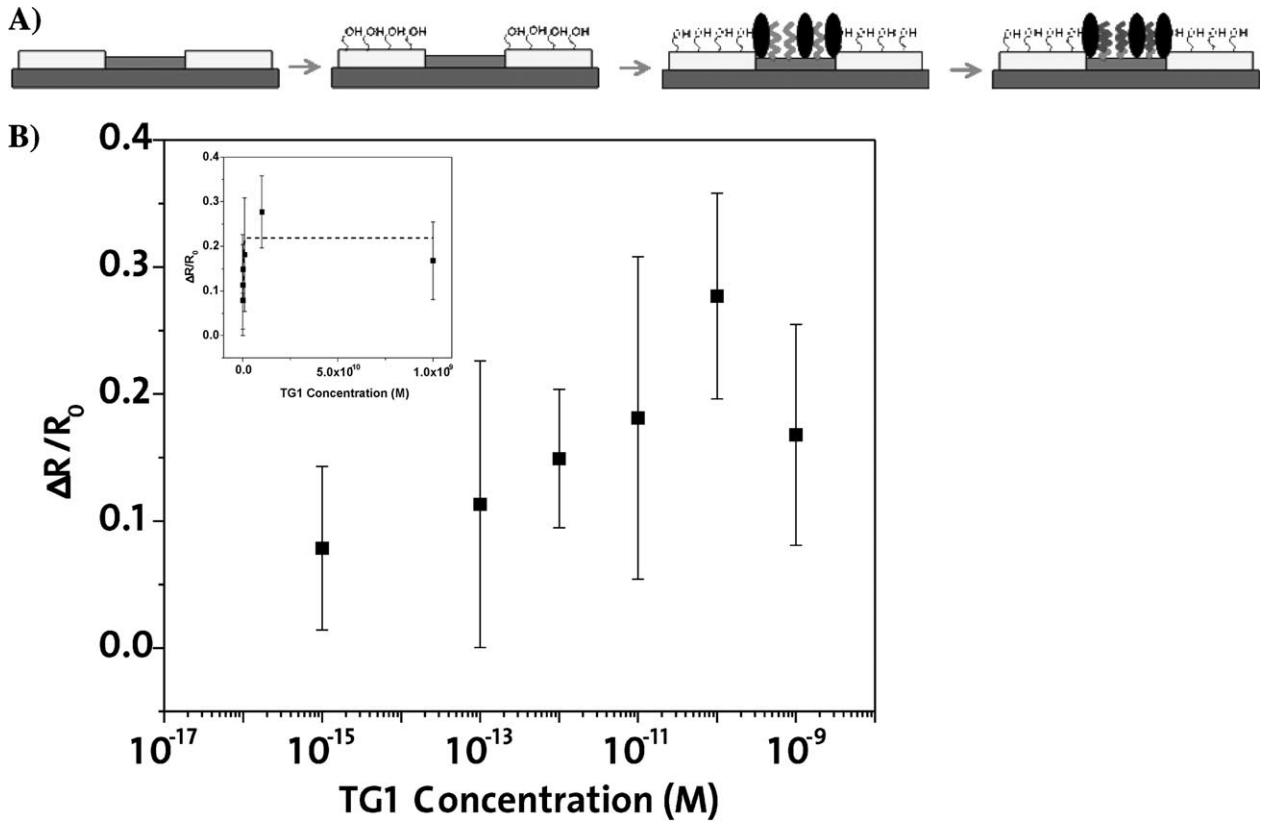

Fig. 1. A) Schematic of the sensor showing different steps involved in the sensor fabrication starting with a single nanowire connected between a pair of gold microfabricated electrodes followed by blocking of gold with mercaptohexanol, followed by immobilization of probe ssDNA on nanowire surface using the linker chemistry explained in Scheme 1 and blocking done using BSA. Finally the functionalized sensor is exposed to the target complementary ssDNA to form a double stranded DNA. B) Response of single Ppy nanowire sensor with thiolated 19 bp probe DNA immobilized on the nanowire surface using SMPB linker using 2-steps ($n=4$) protocol towards sequential exposure to increasing concentrations of the perfectly complementary DNA sequence. (Inset shows the corresponding calibration plot on linear scale) ('n' is the number of sensors)

Ppy nanowire and unfunctionalized gold surface. The devices blocked with BSA without the probe DNA (negative control) showed distinctly lower response [$\Delta R/R_0 = 0.01 \pm 0.056$ ($n=4$ sensors, averaged over all the target concentrations), data not shown] towards TG1 compared to functionalized sensors (Figure 2B). When compared, this work function modulation based sensor showed much better sensitivity, detection limit (~10^{-16} M TG1), operating range (~10^{-16} to 10^{-10} M TG1) and sensor to sensor reproducibility over gating effect based sensors described earlier. From the above results it can be inferred that the extent of probe DNA immobilization has pronounced effect on the sensitivity of both the sensor configurations and the work function difference modulation based sensor was more reliable than gating effect based sensor in terms of the sensitivity, dynamic range and reproducibility.

Figure 3 illustrates the ability of this sensor to discriminate mismatched targets, i.e. selectivity was evaluated using single, double and triple base pair mismatches viz MU2, MU12 and MU123. A very low response for mismatched sequences compared to perfectly complementary TG1 sequence demonstrates the sensor's capability to discriminate between perfectly complementary target sequence and sequences with even a single base pair mismatch even at room temperature. This is very important for application involving detection of SNPs such as breast cancer gene sequence detection demonstrated here. Specifically, distinction between MU2 and TG1 achieved using our sensor has very important implication from real application point of view as the MU2 sequence represents the normal human gene whereas TG1 is an SNP of MU2.

3.2 Metagenomics – Effect of Probe Length

To demonstrate a broader utility of these sensors, we tested sensors functionalized with probe sequences of varying number of bases. Sensors with 21 bases (PR2) and 36 bases long (PR3) probes incorporating BSA blocking of un-functionalized surfaces were fabricated (these sequences were studied due to their applications in analyzing environmental samples in the on-going metagenomics studies at National Environmental Engineering Research Institute) and their responses towards perfectly complementary target probes TG2 and TG3, respectively, were evaluated. As shown in Figure 4 and comparing to

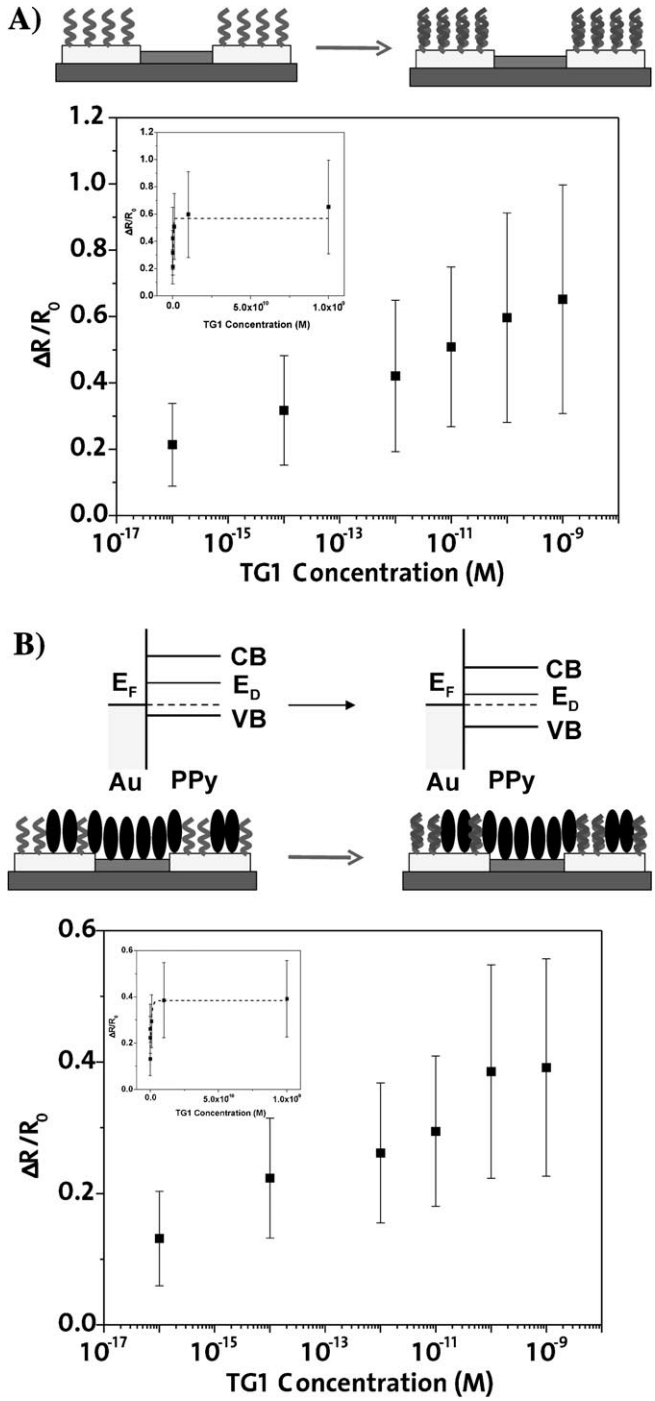

Fig. 2. A) Schematics and calibration plot of the work function modulation based sensors without BSA blocking of nonfunctionalized surfaces ($n=4$). B) Schematics of the energy diagram for the sensor before and after target hybridization along with schematics of the sensor and the calibration plot for work function based sensors with BSA blocking of nonfunctionalized surfaces (■, $n=4$). (Insets show corresponding calibration plots on linear concentration scale)

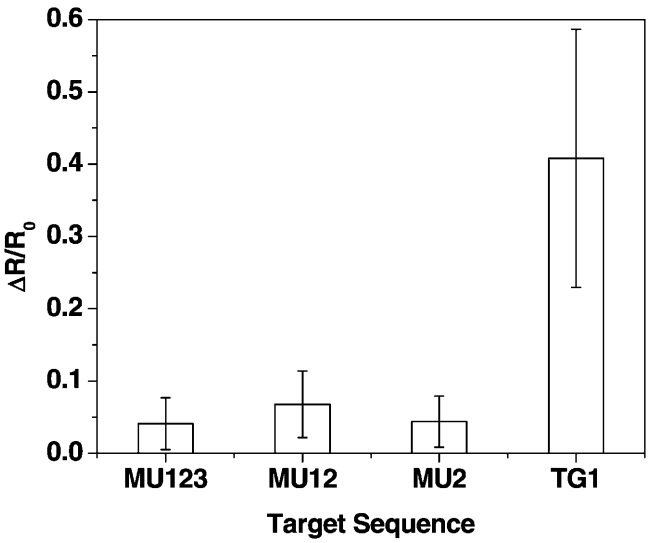

Fig. 3. Response of a single Ppy nanowire DNA sensor with 19 bp DNA probe immobilized on gold surfaces towards target DNA with single (MU2), double (MU12) or triple (MU123) base pair mismatch at 10^{-6} M concentration. For comparison response of the sensor towards perfectly complementary DNA target is plotted from Figure 3C at the same concentration ($n=4$ for each).

the response for the 19 bases long probe sensor (Figure 2B), the response/sensitivity scaled with the length of the DNA probe indicating increase in the extend of metal electrode work function modulation as the DNA chain length was increased. The response of the 36 bases long DNA probe sensor, however, was lowered when an added treatment step of mercaptohexanol (MCH) was employed in the sensor fabrication (Figure 4B). This attenuated response is hypothesized to be a result of the combination of vertical orientation of DNA probe, moving the hybridization site outside the Debye length, and reduced probe density. The supporting arguments for this hypothesis is based on the literature reports that indicate that 1) DNA probes longer than 30 bases upon immobilization on gold nanoparticles results in coiling up of the molecule [39]; 2) thiolated DNA probe can also immobilize on the Au surface through non-specific adsorption due to the interaction between DNA bases and the gold surface [40–50]; 3) treatment with a spacer molecule such as MCH, removes non-specifically adsorbed DNA molecules from the gold surface and at the same time orient the DNA coupled through the thiol-gold bond vertically [40,41]. This result is not only in accordance with previously shown effect of MCH on thiolated DNA immobilization on Au surface [40–46] but also suggests that the control on vertical DNA orientation using spacer molecules or any other technique is not necessary (or in fact detrimental) for even longer sequences. These findings again show the versatility of these sensors for detection of longer sequences without any special treatment. However, high surface coverage of randomly oriented probe DNA have been shown to exhibit lower hybridization efficiency compared to highly oriented, low density DNA probes [42–44,51]. Thus the current sensor design may show saturation in sensitivity for very long DNA sequences necessitating an investigation to establish the limiting

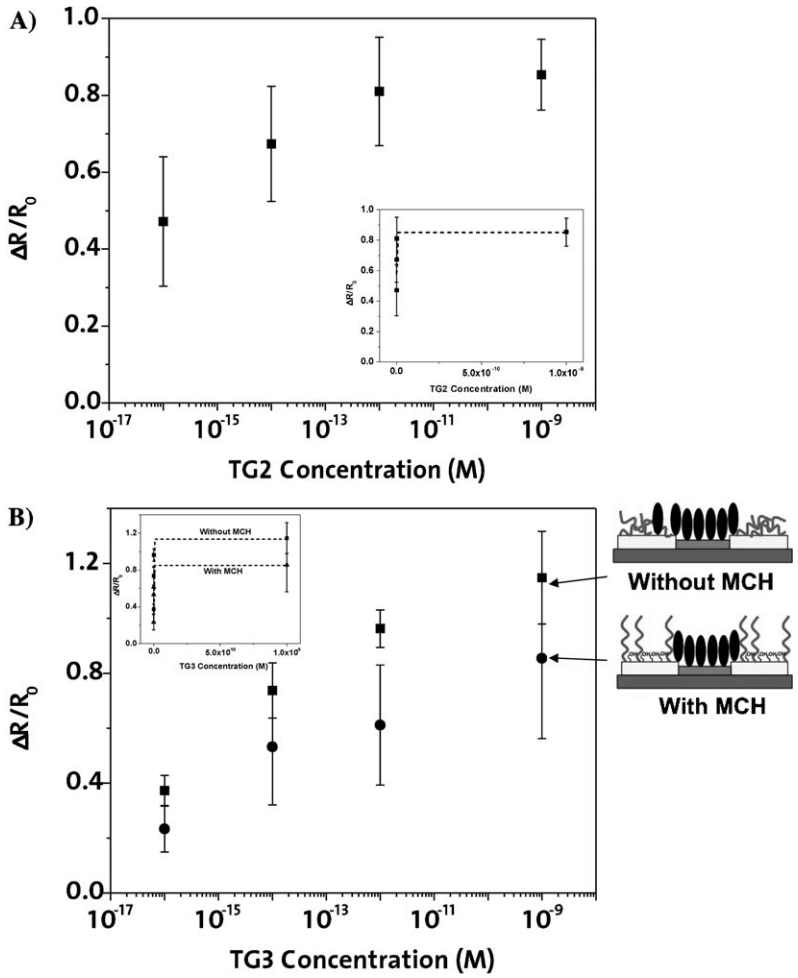

Fig. 4. Response of a single Ppy nanowire DNA sensor with (A) 21 bases long DNA probe ($n=4$) and (B) 36 bases long DNA probe without (■, $n=4$) or with (●, $n=4$) MCH immobilized on gold surfaces upon sequential exposure to increasing concentrations of perfectly complementary DNA targets. Insets: Corresponding calibration plots on linear concentration scale.

length of the DNA sequence that can be detected without the loss of sensitivity, selectivity and sensor to sensor reproducibility.

To our knowledge this is the first example for conducting polymer nanowire FET sensor based on work function modulation. Previously, DNA targets have been detected by monitoring the modulation of conducting polymer film and nanotubes resistance [17–20]. Detection limit of 10^{-16} M (and dynamic range) of target 19 bp DNA concentration achieved using our work-function modulation based sensor exceeds the performance of other conducting polymer nanowire based DNA sensors based on gating effect such as 1) the detection limit of 10^{-9} M of biotinylated 20 bp ssDNA target detection using avidin entrapped single conducting polymer based chemiresistive/FET sensor previously developed by our group [33], 2) 10^{-8} M of target 20 bp DNA achieved using PEDOT (poly(3,4-ethylenedioxythiophene)) nanotubules with physically entrapped probe ssDNA based FET sensor [19] and 3) 10^{-9} M realized with ssDNA probe covalently attached on the surface of poly(pyrrole-3-carboxylic acid) nanotubes [20]. Also the detection limit of the sensor reported here compares with that of 10^{-14} M of target DNA achieved using a PNA functionalized silicon nanowire FET sensor [27] or the detection limit of 10^{-13} M achieved using a gold nanoparticle enhanced DNA detection strategy utilizing carbon nanotube network based FET sensor [52], both working on the principle of gating effect. For carbon-nanotube network based protein [53] and DNA [29] sensors working on the principle of work function difference modulation between the contact gold electrodes and the carbon nanotubes, it has been clearly shown that the Schottky barrier/contact region between the electrodes and the nanotubes is mainly responsible for the signal generation (as against the metal electrode surface away from the contact region) and by incorporating higher density of probe molecules in this region higher sensitivity can be achieved [53]. Such control can be achieved by limiting the Schottky barrier region to a single nanowire-electrode contact as is demonstrated in this study, resulting in the observed sensitivity and limit of detection, as against multiple nanowires/nanotubes [52,29] or a thin semiconducting film in contact with the metal electrodes. Even though,

the calibration curve obtained shows a clear trend of sensor response versus various targets and their concentrations with the current protocol, device to device variations (error bars) of the sensor for current single conducting polymer nanowire based device when compared to gating effect based Si nanowire and CNT sensors mentioned earlier, need further improvement. Batch treatment of the sensors and manual solution dispensing can contribute to bigger error bars in the response curve of our sensors and can be reduced by integrating microfluidic channel for solution handling and delivery along with real-time sensing measurements. Further improvement in the performance of the sensor demonstrated in the current study is expected by applying FET-gate control and/or by fine-tuning the work function difference between the metal electrode and the conducting polymer nanowire. Choice of conducting polymer for nanowire fabrication offers advantages over other nanostructures as simply changing the dopant, level of doping and/or oxidation/reduction state can modulate the work function of the conducting polymer [54]. Additionally, as reported previously, the array architecture of these devices opens the doors for multi-functionality and multianalyte sensing/multiplexing [36].

4 Conclusions

To summarize, for the first time we have constructed a single conducting polymer nanowire based chemiresistive ssDNA sensor working on the principle of Schottky barrier/work function difference modulation between semiconducting nanowire and contact metal electrodes. Schottky barrier modulation based sensor showed better sensing performance than the gating effect based sensor. Limit of detection achieved using Schottky barrier modulation based 19 bp ssDNA sensor was 10^{-16} M of target ssDNA. Detection of target 19 bp breast cancer gene was highly specific down to SNP level discrimination, which makes the sensor highly applicable for medical diagnostic purpose. Additionally, sensitivity of the sensor scaled with the length of the ssDNA bp when longer base pair sequences were used. Vertical orientation of longer (36 bp) probe DNA showed lesser sensitivity compared to random orientation. It is believed that the sensitivity difference is a manifestation of better electrical coupling between the probe ssDNA and the gold electrode resulted from closer proximity of the randomly oriented ssDNA probe to the electrode surface compared to vertical alignment. Detection of longer DNA sequences demonstrates the utility of this sensor for metagenomic/environmental sample detection.

Acknowledgment

We acknowledge the support of Grants GR-83237501 from the *U.S. EPA*, CBET-0617240 from *NSF* and U01ES016026 from *NIH*. HJP is supported through *CSIR*, India, Grant SIP16:4.1.

References

[1] S. Kluber, T. Supali, S. A. Williams, E. Liebau, P. Fischer, *Trans. Roy. Soc. Tropical Med. Hygiene* **2001**, *95*, 169.
[2] G. Ramsey, *Nat. Biotechnol.* **1998**, *16*, 40.
[3] J. J. Storhoff, R. Elghanian, R. C. Mucic, C. A. Mirkin, R. L. Letsinger, *J. Am. Chem. Soc.* **1998**, *120*, 1959.
[4] T. A. Taton, C. A. Mirkin, R. L. Letsinger, *Science* **2000**, *289*, 1757.
[5] J. M. McDonnell, *Curr. Opin. Chem. Biol.* **2001**, *5*, 572.
[6] J. Wang, M. Jiang, E. Palecek, *Bioelectrochem. Bioenergetics* **1999**, *48*, 477.
[7] J. Fritz, M. K. Baller, H. P. Lang, H. Rothuizen, P. Vettiger, E. Meyer, H.-J. Güntherodt, C. Gerber, J. K. Gimzewski, *Science* **2000**, *288*, 316.
[8] T. G. Drummond, M. G. Hill, J. K. Barton, *Nat. Biotechnol.* **2003**, *21*, 1192.
[9] K. Kerman, Y. Morita, Y. Takamura, E. Tamiya, *Electrochem. Commun.* **2003**, *5*, 887.
[10] A. A. Lubin, R. Y. Lai, B. R. Baker, A. J. Heeger, K. W. Plaxco, *Anal. Chem.* **2006**, *78*, 5671.
[11] H. Cai, Y. Wang, P. He, Y. Fang, *Anal. Chim. Acta.* **2002**, *469*, 165.
[12] J. Wang, *Anal. Chim. Acta.* **2003**, *500*, 247.
[13] S. Niu, M. Zhao, R. Ren, S. Zhang, *J. Inorg. Biochem.* **2009**, *103*, 43.
[14] P. He, L. Dai, *Chem. Commun.* **2004**, *3*, 348.
[15] C.-P. Chen, A. Ganguly, C.-H. Wang, C.-W. Hsu, S. Chattopadhyay, Y.-K. Hsu, Y.-C. Chang, K.-H. Chen, L.-C. Chen, *Anal. Chem.* **2009**, *81*, 36.
[16] H. Peng, L. Zhang, C. Soeller, J. Travas-Sejdic, *Biomaterials* **2009**, *30*, 2132.
[17] H. Korri-Yusssoufi, F. Garnier, P. Srivastava, P. Godillot, A. YAssar, *J. Am. Chem. Soc.* **1997**, *119*, 7388.
[18] J. Wang, M. Jiang, A. Fortes, B. Mukherjee, *Anal. Chim. Acta* **1999**, *402*, 7.
[19] K. Krishnamoorthy, R. S. Gokhale, A. Q. Contractor, A. Kumar, *Chem. Commun.* **2004**, *7*, 820.
[20] S. Ko, J. Jang, *Ultramicroscopy* **2008**, *108*, 1328.
[21] J. Fritz, E. B. Cooper, S. Gaudet, P. K. Sorger, S. R. Manalis, *Proc. Natl. Acad. Sci. USA* **2002**, *99*, 14142.
[22] S. Ingebrandt, A. Offenhausser, *Phys. Stat. Sol. A* **2006**, *203*, 3399.
[23] T. Uno, H. Tabata, T. Kawai, *Anal. Chem.* **2007**, *79*, 52.
[24] F. Pouthas, C. Gentil, D. Cote, U. Bockelmann, *Appl. Phys. Lett.* **2004**, *84*, 1594.
[25] J. Hahm, C. M. Lieber, *Nano Lett.* **2004**, *4*, 51.
[26] Z. Li, B. Rajendran, T. I. Kamins, X. Li, Y. Chen, R. S. Williams, *Appl. Phys. A* **2005**, *80*, 1257.
[27] Z. Q. Gao, A. Agarwal, A. D. Trigg, N. Singh, C. Fang, C. H. Tung, Y. Fan, K. D. Buddharaju, J. M. Kong, *Anal. Chem.* **2007**, *79*, 3291.
[28] A. Star, E. Tu, J. Niemann, J.-C. P. Gabriel, C. S. Joiner, C. Valcke, *Proc. Natl. Acad. Sci.* **2006**, *103*, 921.
[29] X. Tang, S. Bansaruntip, N. Nakayama, E. Yenilmez, Y. L. Chang, Q. Wang, *Nano Lett.* **2006**, *6*, 1632.
[30] E. L. Gui, L.-J. Li, K. Zhang, Y. Xu, X. Dong, X. Ho, P. S. Lee, J. Kasim, Z. X. Shen, J. A. Rogers, S. G. Mhaisalkar, *J. Am. Chem. Soc.* **2007**, *129*, 14427.
[31] D. R. Kauffman, A. Star, *Chem. Soc. Rev.* **2008**, *37*, 1197.
[32] I. Heller, A. M. Janssens, J. Männik, E. D. Minot, S. G. Lemay, C. Dekker, *Nano Lett.* **2008**, *8*, 591.

[33] N. Peng, Q. Zhang, C. L. Chow, O. K. Tan, N. Marzari, *Nano Lett.* **2009**, *9*, 1626.
[34] E. S. Forzani, H. Zhang, L. A. Nagahara, I. Amlani, R. Tsui, N. Tao, *Nano Lett.* **2004**, *4*, 1785.
[35] K. Ramanathan, M. A. Bangar, M. Yun, W. Chen, N. V. Myung, A. Mulchandani, *J. Am. Chem. Soc.* **2005**, *127*, 496.
[36] M. A. Bangar, D. J. Shirale, W. Chen, N. V. Myung, A. Mulchandani, *Anal. Chem.* **2009**, *81*, 2168.
[37] H. Yoon, J.-H. Kim, N. Lee, B.-G. Kim, J. Jang, *ChemBioChem.* **2008**, *9*, 634.
[38] S. B. Tolani, M. Craig, R. K. Delong, K. Ghosh, A. K. Wanekaya, *Anal. Bioanal. Chem.* **2009**, *393*, 1225.
[39] W. J. Parak, T. Pellegrino, C. M. Micheel, D. Gerion, S. C. Williams, A. P. Alivisatos, *Nano Lett.* **2003**, *3*, 33.
[40] K. Arinaga, U. Rant, M. Tornow, S. Fujita, G. Abstreiter, N. Yokoyama, *Langmuir* **2006**, *22*, 5560.
[41] R. Levicky, T. M. Herne, M. J. Tarlov, S. K. Satija, *J. Am. Chem. Soc.* **1998**, *120*, 9787.
[42] T. M. Herne, M. J. Tarlov, *J. Am. Chem. Soc.* **1997**, *119*, 8916.
[43] R. Lao, S. Song, H. Wu, L. Wang, Z. Zhang, L. He, C. Fan, *Anal. Chem.* **2005**, *77*, 6475.
[44] A. B. Steel, T. M. Herne, M. J. Tarlov, *Anal. Chem.* **1998**, *70*, 4670.
[45] A. Kick, M. Bönsch, K. Kummer, D. V. Vyalikh, S. L. Molodtsov, M. Mertig, *J. Electron Spectrosc. Rel. Phenom.* **2009**, *172*, 36.
[46] R. Georgiadis, K. P. Peterlinz, A. W. Peterson, *J. Am. Chem. Soc.* **2000**, *122*, 3166.
[47] D. Y. Petrovykh, H. Kimura-Suda, M. J. Tarlov, L. J. Whitman, *Langmuir* **2004**, *20*, 429.
[48] J. J. Storhoff, R. Elghanian, C. A. Mirkin, R. L. Letsinger, *Langmuir* **2002**, *18*, 6666.
[49] L. M. Demers, M. Ostblom, H. Zhang, N.-H. Jang, B. Liedberg, C. A. Mirkin, *J. Am. Chem. Soc.* **2002**, *124*, 11248.
[50] H. Kimura-Suda, D. Y. Petrovykh, M. J. Tarlov, L. J. Whitman, *J. Am. Chem. Soc.* **2003**, *125*, 9014.
[51] A. W. Peterson, R. J. Heaton, R. M. Georgiadis, *Nucleic Acids Res.* **2001**, *29*, 5163.
[52] X. Dong, C. M. Lau, A. Lohani, S. G. Mhaisalkar, J. Kasim, Z. Shen, X. Ho, J. A. Rogers, L.-J. Li, *Adv. Mater.* **2008**, *20*, 2389.
[53] H. R. Byon, H. C. Choi, *J. Am. Chem. Soc.* **2006**, *128*, 2188.
[54] J. Janata, M. Josowicz, *Nat. Mater.* **2003**, *2*, 19, and references therein.

